

Improving the Performance of Gas Turbine Power Plant by Modified Axial Turbine

Hakim T. Kadhim, Faris A. Jabbar, Aldo Rona, Audrius Bagdanaviciu

Abstract—Computer-based optimization techniques can be employed to improve the efficiency of energy conversions processes, including reducing the aerodynamic loss in a thermal power plant turbomachine. In this paper, towards mitigating secondary flow losses, a design optimization workflow is implemented for the casing geometry of a 1.5 stage axial flow turbine that improves the turbine isentropic efficiency. The improved turbine is used in an open thermodynamic gas cycle with regeneration and cogeneration. Performance estimates are obtained by the commercial software Cycle – Tempo. Design and off design conditions are considered as well as variations in inlet air temperature. Reductions in both the natural gas specific fuel consumption and in CO₂ emissions are predicted by using the gas turbine cycle fitted with the new casing design. These gains are attractive towards enhancing the competitiveness and reducing the environmental impact of thermal power plant.

Keywords—Axial flow turbine, computational fluid dynamics, gas turbine power plant, optimization.

I. INTRODUCTION

WITH sustained increases in environmental concerns, world-wide population, demand for electrical energy, and cost of fuel, advances in the design of gas cycle power plants and of their individual components are required to improve the performance of the cycle and reduce both of the natural gas used for driving the cycle and the CO₂ emissions.

Gas turbine cycle power plants are used extensively for power generation across the world. Many retrofit technologies are available to improve the efficiency and/or the power output of a power plant running on the basic Brayton cycle. Agarwal et al. [1] sequentially retrofitted a gas turbine steam injection system and an inlet air cooling heat exchanger to a simple gas turbine power generator. Adding these features was shown to substantially improve the power output from 30 MW to up to 48.25 MW. This also reduced the thermal pollution and energy waste of the plant.

Cogeneration can be used for producing heat and power for local district heating in an efficient way [2]. However, achieving a turbine exhaust temperature that is sufficient for the process of steam production requires either a low boiler pressure ratio or a high turbine outlet temperature. Therefore, to achieve better thermodynamic performance, a more

complex power unit is required.

Another approach to adding thermodynamic performance to a simple cycle featuring a modest cycle overall pressure ratio is by regeneration. A heat exchanger transfers heat from the turbine exhaust stream to the compressor outlet stream, thereby reducing the amount of heat added in the combustor to achieve a target turbine inlet temperature. Cogeneration and regeneration can be combined together. Kumar et al. [3] investigated the efficiency of a gas turbine cogeneration cycle fitted with a heat recovery system (regenerator). They found that combining regeneration and co-generation improved the cycle performance compared to a simple gas turbine cycle, provided the heat output from co-generation can be considered as useful energy output in the cycle performance analysis.

A further way for improving the performance of a thermal power plant is by improving the isentropic efficiency of the axial turbine component of the thermodynamic cycle. This can be achieved by mitigating the secondary flow losses in the turbine through-flow. The reduction of turbine secondary flow losses is an active research area, as these losses represent approximately 40% to 50% of the estimated total aerodynamic losses in an axial turbine [4]. Thus, reducing these losses results in an increase in the turbine efficiency. Turbine secondary flows and their causes are reviewed in references [5]-[8]. Mitigating techniques for secondary flows are reviewed in Langston [9] and in Kadhim and Rona [10], where endwalls are highlighted as a promising approach.

The use of non-axisymmetric endwalls has shown to be a robust method for enhancing the performance of axial turbines in power generation. This technique controls the onset and the growth of secondary flows by surface shape changes at the hub and/or at the casing. These surface shape changes are designed using computational fluid dynamics (CFD) coupled with a variety of optimization methods [11]. Shahpar et al. [12] presented a new optimization methodology based on adjoint sensitivity analysis and trust-based dynamic response surface modeling to improve the performance of a high pressure turbine stage, using multi-row 3-D CFD simulations. The results showed that the turbine stage efficiency can be significantly enhanced using a local non-axisymmetric endwall design upstream of the rotor leading edge in the mid-passage. Kim et al. [13] optimized the profiled shroud and the hub of a one-stage high-pressure transonic turbine. These endwall modifications improved the stage isentropic efficiency by 0.39%, using both the optimized shroud and hub, while a 0.4% efficiency gain was achieved from the application of the optimized shroud alone.

In this paper, a power cycle featuring regeneration and

H. T. Kadhim, PhD student, A. Rona, Associate Professor, A Bagdanavicius, Lecturer, are with the Department of Engineering, University of Leicester, University Road, LE1 7RH, Leicester, UK. (e-mail: hkk10@le.ac.uk, ar45@le.ac.uk, ab746@le.ac.uk).

H. T. Kadhim, F. A. Jabbar are Lecturers Mechanical Department, Al-Dewaniyah Technical Institute, Al-Furat Al-Awsat Technical University, Iraq (e-mail: hakim.kadhim@yahoo.com, farisabdhani1971@yahoo.com).

cogeneration is modelled with a power turbine fitted with a contoured casing endwall. A turbine casing design is used, which is based on a surface definition method that draws from the natural path of the typical secondary flow features over the casing. The changes in the cycle performance are investigated by varying the isentropic efficiency of the turbine cycle. The improved turbine with the optimized casing design is run at design and off design conditions. The commercial software Cycle – Tempo is used to evaluate the change in the thermodynamic cycle performance. This includes the improvements in the natural gas specific fuel consumption and the reduction in CO₂ emissions.

II. GAS TURBINE POWER PLANT WITH REGENERATION AND COGENERATION

A standard gas turbine unit is fitted with regeneration and cogeneration units as shown in Fig. 1. The base cycle (open Bryton cycle) is made up of the compressor, the combustor, and the turbine. The base cycle is modified by adding a

regenerator, as shown in Fig. 1. Specifically, air enters the cycle from the inlet, labelled as 1 in Fig. 1. It is then compressed through a multi-stage compressor, labelled as item 2. After the compression stage, air enters the regenerator, labelled as item 5. The regenerator increases the air temperature using heat transferred from the combustion products that outflow from the turbine. This heated air then enters the combustor, labelled as item 3 in Fig. 1, where its temperature further increases. In the current model, combustion is achieved by burning natural gas. High pressure and temperature gases then expand through the power turbine, which is labelled as item 6 in Fig. 1, and produce work output. The mechanical work from the turbine is converted to electrical power by a generator, labelled as G in Fig. 1. After passing through the regenerator, item 5 in Fig. 1, the combustion products pass through a heat recovery steam generator, item 8 in Fig. 1, in which heat is transferred to pressurized water to generate steam.

Open Science Index, Mechanical and Mechatronics Engineering Vol:12, No:6, 2018 waset.org/Publication/10009336

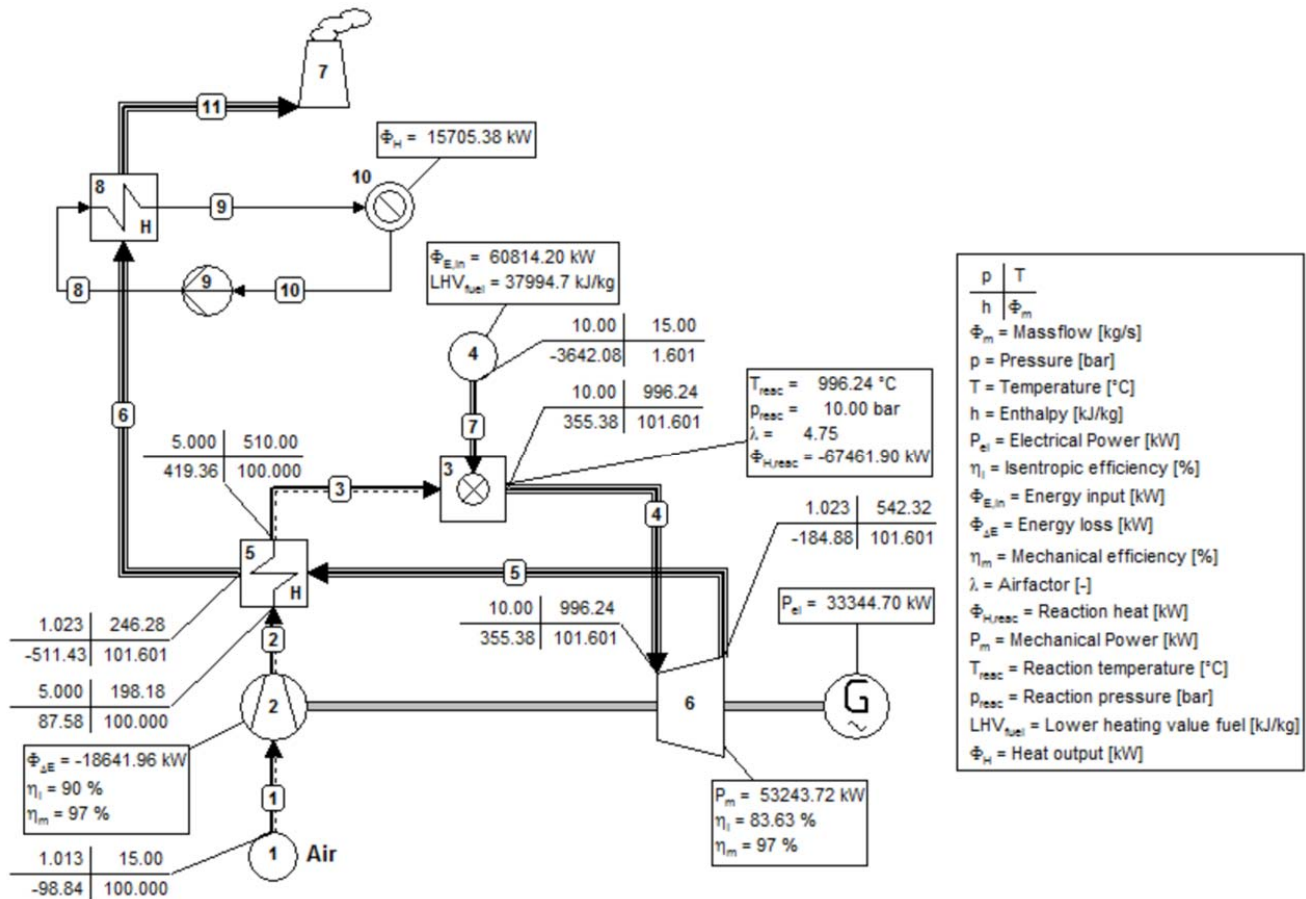


Fig. 1 Gas turbine cycle with regeneration and cogeneration processes using the optimized casing modelled with Cycle-Tempo

III. POWER PLANT CYCLE MODELLING

In this work, a gas turbine modified with an optimized profiled casing design is used to improve the performance of the regenerative gas turbine cogeneration plant shown in Fig. 1. The thermodynamic cycle of Fig. 1 is modelled using the

commercial software Cycle-Tempo [14]. The natural gas used in the combustor, item 3 in Fig. 1, is taken as standard natural gas having the composition of Table I, with a low calorific value LHV_{fuel} of 37,994.7 kJ/kg [14]. Fig. 1 shows the change in the working fluid state at different points through the cycle

by 2×2 matrix callouts. Each matrix reports, from top left to bottom right, the pressure (Bar), temperature (Celsius), the specific enthalpy (kJ/kg), and the mass flow rate (kg/s) of the working fluid. Callout matrices for the inlet air and for the inlet fuel in Fig. 1 define the cycle inflow conditions at the design point.

To evaluate the cycle performance change, two Cycle-Tempo models are built at the design and off-design operating conditions for the gas turbine.

TABLE I
 STANDARD NATURAL GAS COMPONENTS

Natural gas component	Chemical symbols	Mole Fraction (%)
Nitrogen	N ₂	14.32
Oxygen	O ₂	0.01
Carbon dioxide	CO ₂	0.89
Methane	CH ₄	81.29
Ethane	C ₂ H ₆	2.87
Propane	C ₃ H ₈	0.38
i-Butane	C ₄ H ₁₀	0.15
n-Butane	C ₄ H ₁₂	0.04
i-Pentane	C ₅ H ₁₄	0.05

IV. CFD OPTIMIZATION OF THE MODIFIED AXIAL TURBINE

The 1.5 stage Aachen Turbine [15] is used as the baseline power turbine to develop an improved turbine featuring a non-axisymmetric casing. Detailed measurements and design data of the Aachen Turbine are given in [15]. The turbine is improved by applying a non-axisymmetric casing to the first

stator. A schematic view of the Aachen Turbine and of its basic through-flow geometry at the blade mid-span is shown in Fig. 2.

The time-averaged flow through the turbine is modelled as pitchwise-periodic, by performing a Reynolds Averaged Navier-Stokes (RANS) turbulent flow simulation through one turbine flow passage and taking the predictions as applicable pitchwise to all the passages. Mixing planes are used at the rotor-stator interfaces. The flow predictions through the baseline power turbine were validated [16] against corresponding measurements of rotor and stator exit velocity components and of flow angles taken at the Rheinisch-Westfälische Technische Hochschule, Aachen [15]. The sensitivity of the predictions to the spatial resolution of the computational grid were investigated [16] by means of the Grid Convergence Index evaluated on progressively refined meshes. Furthermore, the sensitivity of the predictions to the choice of the turbulence closure model was assessed by comparing predictions obtained using the RNG $k - \epsilon$ and the $k - \omega$ Shear Stress Transport (SST) turbulence closure models [16]. This analysis provided evidence that an appropriately space-resolved mesh with a near-wall resolution $y^+ = 1$ combined with the $k - \omega$ SST model gives satisfactory predictions. Specifically, it was found that the changes in the predicted total pressure loss by further refining the mesh were one order of magnitude lower than the corresponding changes induced by the endwall modifications presented later on. As such, the model was deemed sufficient for the purpose of optimizing the turbine endwall.

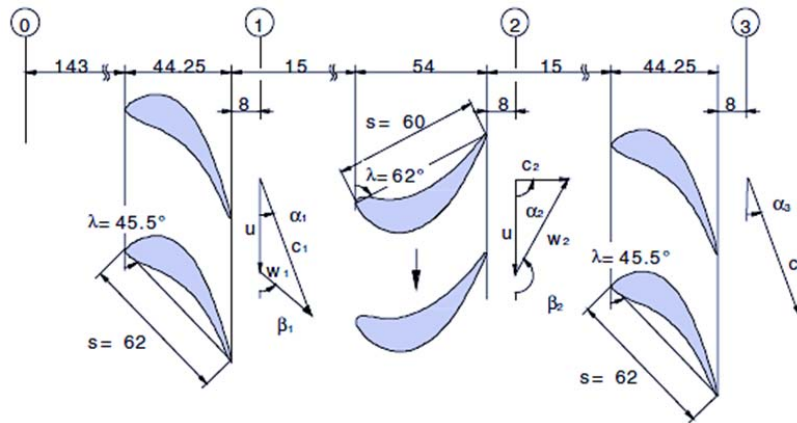


Fig. 2 Schematic of the Aachen Turbine on the cascade plane [15]. All lengths are stated in mm

Having obtained a satisfactory Computational Fluid Dynamic simulation of the flow through the baseline Aachen Turbine, with axisymmetric end-walls, the numerical model is used to investigate variants of the baseline model, in which the axisymmetric casing is replaced by a non-axisymmetric wall, designed following the guide groove approach [17]. The non-axisymmetric wall is a parametrized surface, the parameters of which require optimization. This parametric optimization is achieved by application of the workflow of Fig. 3. The design optimization workflow of Fig. 3 is developed and implemented by the Automated Process and Optimization

Workbench (APOW) software. A profiled casing surface is generated in MATLAB and then imported in ANSYS ICEM CFD as a non-uniform radial B-spline (NURBS) surface. Similar computational mesh generation parameters are used in ANSYS ICEM CFD as for the validated baseline geometry to obtain a similar mesh quality. The unstructured mesh is translated to OpenFOAM 3.2 Extend and the numerical solution is iterated to convergence, as assessed by the reduction in the residuals by 10^{-5} of their value at the onset of the computation. The stage total pressure loss coefficient is selected as the objective function, which is calculated as a

pitchwise and radially averaged quantity based on: $C_{ptr} = (P_{t0} - P_{t2}) / (P_{t2} - P_2)$, where subscript 0 denotes the stator inlet plane and subscript 2 denotes the rotor exit plane.

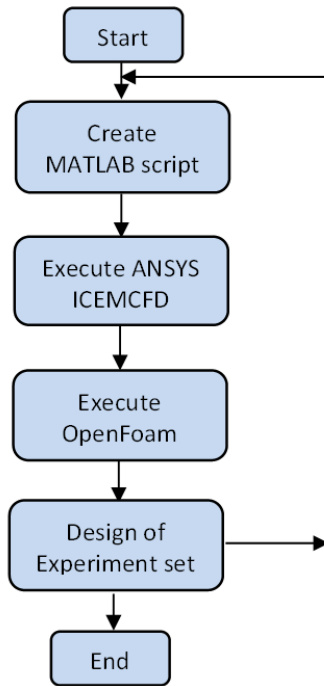


Fig. 3 Optimization workflow in APOW

Fig. 4 gives a wire-mesh graphical rendering of the non-axisymmetric stator casing, which features the guide groove [17] running from near the leading edge of the rightmost blade in Fig. 4, to the blade row passage trailing edge. A lighter tone in Fig. 4 sets the groove apart from the remainder of the axisymmetric casing, which is shown in a darker shade. Whereas the casing surface is defined as a NURBS graphical object, which makes it nearly free-form, a hierarchy of design constraints is built to constrain the non-axisymmetric surface to shapes that can both be manufactured and that have a reasonable promise of controlling the casing secondary flows. Specifically, the groove centerline path in the cascade plane is defined [17] by a pitchwise interpolation of the blade root profiles of pitchwise consecutive blades offset from the blade root. This approach makes this design compatible with root fillets, which often feature in turbomachinery blades (but not used on the Aachen Turbine). The groove width normal to its path is varied linearly from the groove leading edge to the groove trailing edge. The groove maximum depth is set at 3 mm, which is selected in consideration of not unduly weakening the mechanical strength of the casing wall. The axial position of the groove maximum depth h_o and the groove trailing edge width w_{te} are set as free parameters and optimized by the workflow of Fig. 1. In this application of APOW, the task is therefore to perform a bi-variate optimization in the groove parameter space (h_o, w_{te}) . The design of experiment DoE is used to sample this design space with the optimal Latin hypercube (OLH) design method.

Whereas OLH gives a good statistical coverage of the design space, running the CFD model at specific combinations of (h_o, w_{te}) produces a discrete, sampled response. Optimized (h_o, w_{te}) values are obtained by fitting a continuous response function to the sampled response, using Kriging. The Kriging model generates a response function that is a continuous surface, which is more computationally efficient to survey for minima. From this analysis, an endwall casing shape is identified, using $h_o = 0.74$ of the groove path length and $w_{te} = 0.05$ radians, that improves the turbine isentropic efficiency from 82.5%, with an axisymmetric casing, to 83.63%, with the non-axisymmetric casing.

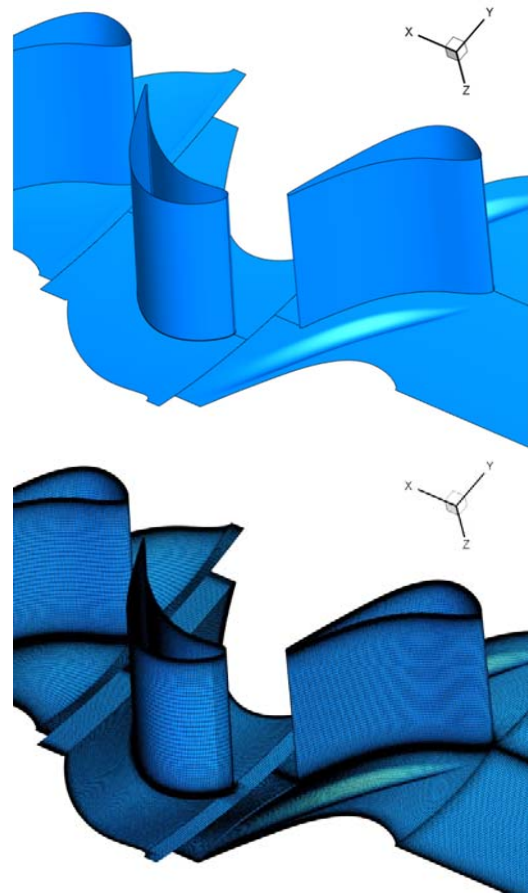


Fig. 4 Non-axisymmetric optimized casing design imported in ICEM CFD

V. CYCLE PERFORMANCE WITH MODIFIED AXIAL TURBINE

The thermodynamic cycle of Fig. 1 is investigated on the basis of classical cycle performance parameter. These parameters include the thermal efficiency of the cycle η_{th} , which is defined as the ratio of the net work output W_{net} to the energy input (heat supplied) Q_f . $W_{net} = W_{turbine} - W_{compressor}$ and $Q_f = \phi_{fuel} \times LHV_{fuel}$, where ϕ_{fuel} is the mass of the fuel supplied. The specific fuel consumption of a thermal system is defined as $SFC = \phi_{fuel} / W_{net}$.

The generation efficiency of a thermal system η_G is the ratio of the electrical energy output (useful energy extracted), W_{el}

to the total heat supplied Q_f , that is $\eta_G = W_{el}/Q_f$. The relationship between W_{net} and W_{el} is $W_{el} = \epsilon_{el} \times W_{net}$, where ϵ_{el} is the system effectiveness of the electrical generation. The power to heat ratio (R_{PH}) is the ratio of the electrical power output, P_{el} to the process heat rate input \dot{Q}_f of the thermal system and it is computed as $R_{PH} = P_{el}/\dot{Q}_f$.

The performance parameters of the thermodynamic cycle of Fig. 1 are improved by improving the stage isentropic efficiency of the axial turbine as shown in Table II. At off design conditions, a comparable improvement can be obtained, where the thermal efficiency increases by 2.91% with the application of the non-axisymmetric endwall. This produces a reduction in the amount of the natural gas that is consumed by the gas turbine cycle.

VI. REDUCTION IN CO₂ EMISSIONS

The CO₂ emissions of from the thermodynamic cycle of

Fig. 1 are studied with the baseline turbine and with the turbine upgraded by the endwall treatment, under a constant mechanical work output to the generator. This condition is met by adjusting the natural gas flow rate between Cycle-Tempo simulations. LHV_{fuel} is also kept constant among the simulation.

The CO₂ generated by the cycle is estimated on the basis of the natural gas flow rate, adjusted to maintain the same mechanical work output, which is assumed to be converted into heat input through by the following stoichiometric chemistry species balance:

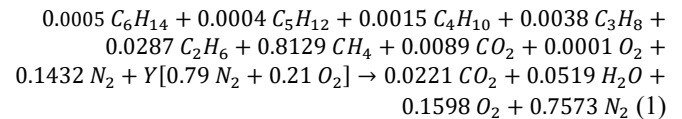


TABLE II
PERFORMANCE PARAMETERS OF THE REGENERATIVE GAS TURBINE COGENERATION PLANT AT DESIGN AND AT OFF DESIGN CONDITIONS

Performance parameters	Design conditions		Off design conditions	
	Baseline Cycle	Cycle with modified turbine	Baseline Cycle	Cycle with modified turbine
Cycle thermal efficiency (%)	53.52	54.69	51.524	52.494
Power generation efficiency (%)	52.46	0.536	50.51	51.46
Specific fuel consumption (kg/kWh)	0.1731	0.1694	0.1797	0.1762
Turbine work (kW)	52524.30	53243.72	51289.18	51887.64
Comperosser work (kW)	19218.52	19218.52	19218.52	19218.52
Net work output (kW)	33305.78	34025.2	32070.66	32669.12
Electric work done (kW)	32639.66	33344.7	31429.25	32015.74
Power to heat ratio	0.524	0.536	0.505	0.511

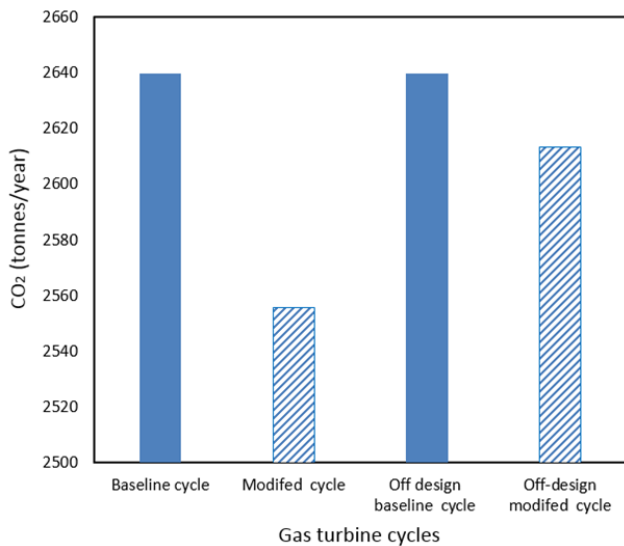


Fig. 5 Effect of improving the power turbine performance on the annual CO₂ emissions of the cycle, at design and off-design

The molar weights of NG and the CO₂ are 18.5978 kg/kmol and 44.0 kg/kmol respectively. Therefore, 1 kg of NG generates 0.05229 kg of CO₂.

At its design point, the thermal cycle of Fig. 1 with the baseline power turbine uses a mass flow rate of fuel of 1.601

kg/s. Based on the correspondence of 1 kg of NG to 0.05229 kg of CO₂, this cycle releases CO₂ at the rate of 0.08371 kg/s. This is equivalent to 2639.87 tonnes of CO₂/year.

The thermal cycle of Fig. 1 fitted with the improved power turbine is able to deliver the same mechanical work with a 2.124% reduction in fuel consumption. This corresponds to a saving of 55.82 tonnes of CO₂/year.

As the thermal cycle of Fig. 1 with the improved power turbine is run off design, the saving in fuel reduces to 1.832% compared to the same cycle that uses the baseline turbine. This could still save 48.36 tonnes of CO₂/year if the cycle were continuously at this set point.

Fig. 5 gives a graphical representation of the above stated savings in CO₂, clearly showing a potential environmental advantage in using the power turbine with the contoured casing endwall, both at design and off design.

VII. EFFECT OF COMPRESSOR INLET TEMPERATURE

Fig. 6 investigates the effect of changing the inlet air temperature on the thermal efficiency and on the power to heat ratio of the cycle shown Fig. 1. Results for both the cycle that uses the baseline turbine and for the cycle modelled with a turbine with a contoured casing endwall are presented. As the air inlet temperature increases, both the thermal efficiency and the power to heat ratio monotonically decrease, for all configuration. This trend is consistent with the fundamental

behavior of all thermal cycles, which can be described by reference to the Carnot cycle efficiency, which depends on the lowest to highest temperature ratio in the cycle. In this case, the inlet air represents the lowest cycle temperature and, hence, increasing this value reduces the lowest to highest temperature ratio and hence the cycle maximum theoretical efficiency (the Carnot efficiency). The efficiency and the power to heat ratio of the cycle with the contoured enwall are consistently above the corresponding values predicted by the simulation that used the baseline turbine in the cycle.

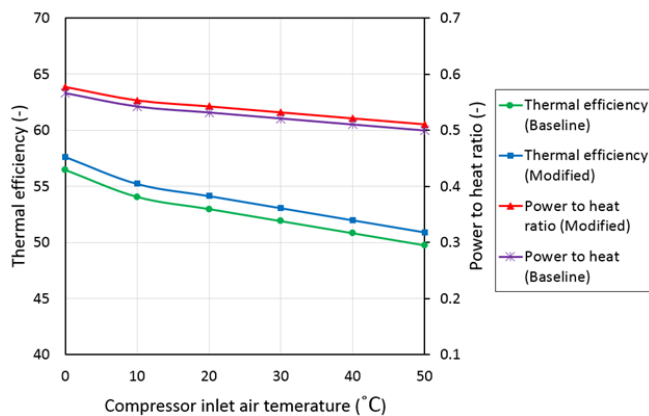


Fig. 6 Effect of compressors inlet air temperature on the thermal efficiency and on the power to heat ratio at design condition

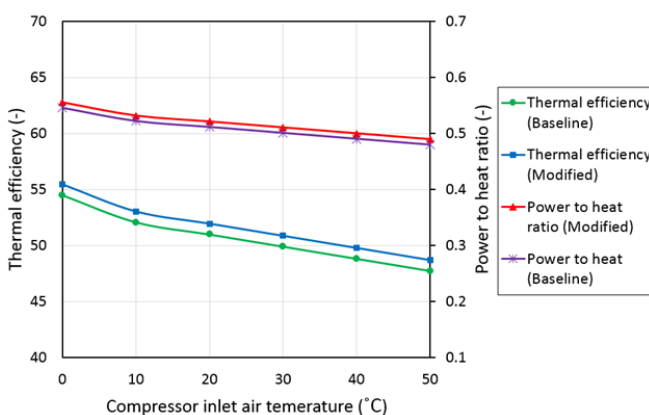


Fig. 7 Effect of compressors inlet air temperature on the thermal efficiency and on the power to heat ratio at off design condition

Fig. 7 presents the corresponding results with the cycle operated off-design. These display the same trends as for the design point cycle operation predictions shown in Fig. 6.

VIII. CONCLUSION

Numerical simulations identify attractive improvements to an open thermodynamic cycle with co-generation and regenerative heating. These improvements are obtained by using a power turbine with a non-axisymmetric enwall of design.

Two models are built, based on the change in isentropic efficiency of the power turbine that is obtained by the endwall treatment. These models predict an increase in the

performance parameters of the gas turbine cycle by increasing the turbine stage isentropic efficiency.

Estimates of the direct environmental advantage of utilizing the casing design technique in a representative gas turbine cycle are provided. These show that consistent savings, both in fuel and in CO₂ emission, are obtained with the power turbine featuring enwall treatments. These savings persist at off-design as well as over a range of inlet air temperatures. These results are encouraging, as the persistence of the performance advantages at off design and for different air inlet temperatures model more closely the current operation of power plants, which experience greater load variability due to the progressive introduction of intermittent renewable energy sources on the grid. They also reflect geographical and seasonal variations of inlet air through the power generation sector.

Further indirect advantages will emerge from savings in both the processing and the transportation expenses of the fuel used by the gas turbine power plant as well as savings in the treatment of the exhaust gasses before discharging to the atmosphere.

ACKNOWLEDGMENT

This research used the ALICE high performance computing facility at the University of Leicester. Graphical rendering software licenses were originally acquired with EPSRC support on Grant GR/N23745/01. The Higher Committee for Education Development in Iraq (HCED) is acknowledged. The supply of experimental data for the 1.5 stage axial flow turbine "Aachen Turbine" under license by RWTH Aachen is gratefully acknowledged.

REFERENCES

- [1] Agarwal, S., Kachhwaha, S., Mishra, R., 2011, "Performance improvement of a simple gas turbine cycle through integration of inlet air evaporative cooling and steam injection."
- [2] Irimescu, A., Lelea, D., 2010, "Thermodynamic analysis of gas turbine powered cogeneration systems."
- [3] Kumar, A., Kachhwaha, S., Mishra, R., 2010, "Thermodynamic analysis of a regenerative gas turbine cogeneration plant."
- [4] Schobeiri, M., 2005, *Turbomachinery flow physics and dynamic performance*, Springer, Germany.
- [5] Coull, J. D., 2017, "Endwall loss in turbine cascades," *Journal of Turbomachinery*, 139(8) pp. 081004-081012.
- [6] Ligrani, P., Potts, G., Fatemi, A., 2017, "Endwall aerodynamic losses from turbine components within gas turbine engines," *Propulsion and Power Research*, 6(1) pp. 1-14.
- [7] Wang, S.-s., Sun, H., Di, J., Mao, J.-r., Li, J., Cai, L.-x., 2014, "High-resolution measurement and analysis of the transient secondary flow field in a turbine cascade," *Proceedings of the Institution of Mechanical Engineers, Part A: Journal of Power and Energy*, 228(7) pp. 799-812.
- [8] Wang, H. P., Olson, S. J., Goldstein, R. J., Eckert, E. R. G., 1997, "Flow visualization in a linear turbine cascade of high performance turbine blades," *Journal of Turbomachinery*, 119(1) pp. 1-8.
- [9] Langston, L., 2001, "Secondary flows in axial turbines—a review," *Annals of the New York Academy of Sciences*, 934(1) pp. 11-26.
- [10] Kadhim, H. T., Rona, A., 2017, "Perspectives on the Treatment of Secondary Flows in Axial Turbines," *Energy Procedia*, 142 pp. 1179-1184.
- [11] Kadhim, H. T., Rona, A., 2018, "Design optimization workflow and performance analysis for contoured endwalls of axial turbines," *Energy*, 149 pp. 875-889.
- [12] Shahpar, S., Caloni, S., de Prieaglle, L., 2017, "Automatic design optimization of profiled endwalls including real geometrical effects to

- minimize turbine secondary flows," *Journal of Turbomachinery*, 139(7) pp. 071010-071011.
- [13] Kim, I., Kim, J., Cho, J., Kang, Y.-S., 2016, "Non-axisymmetric endwall profile optimization of a high-pressure transonic turbine using approximation model," In: *ASME Turbo Expo 2016: Turbomachinery Technical Conference and Exposition*, ASME Paper GT2016-57970.
- [14] Woudstra, N., Van der Stelt, T., 2002, "Cycle-Tempo: a program for the thermodynamic analysis and optimization of systems for the production of electricity, heat and refrigeration," In: *Energy Technology Section*, Delft University of Technology.
- [15] Walraevens, R. E., Gallus, H. E., 1997, "European Research Community on Flow Turbulence and Combustion; ERCOFTAC SIG on 3D turbomachinery flow predictions; Test Case 6: 1-1/2 stage axial flow turbine," In: *Seminar and Workshop on 3D Turbomachinery flow prediction*.
- [16] Kadhim, H. T., 2018, "Effect of non-axisymmetric casing on flow and performance of an axial turbine," PhD thesis, University of Leicester, United Kingdom.
- [17] Kadhim, H., Rona, A., Gostelow, J. P., Leschke, K., 2018, "Optimization of the non-axisymmetric stator casing of a 1.5 stage axial turbine," *International Journal of Mechanical Sciences*, 136 pp. 503-514.